DOI: 10.1021/ma901607w

Macromolecules
ARTICLE

Room-Temperature, Aqueous-Phase Fabrication of Poly(methacrylic acid) Brushes by UV-LED-Induced, Controlled Radical Polymerization with High Selectivity for Surface-Bound Species

Raphael Heeb, Robert M. Bielecki, Seunghwan Lee, and Nicholas D. Spencer*

Laboratory for Surface Science and Technology, Department of Materials, ETH Zurich, Wolfgang-Pauli-Strasse 10, CH-8093 Zurich, Switzerland

Received July 22, 2009; Revised Manuscript Received September 4, 2009

ABSTRACT: Poly(methacrylic acid) (PMAA) brushes were grafted from Si/SiO_2 substrates by means of immobilized-photoiniferter-mediated controlled radical polymerization. The employed UV setup was based on ultraviolet light-emitting diodes (UV-LEDs), which allowed for a precise control of the brush height with irradiation time, as observed by *in situ* quartz crystal microbalance experiments with dissipation monitoring (QCM-D). In contrast to many alternative approaches, it was shown that the novel UV source in combination with a photoiniferter renders lengthy postcleaning steps of the synthesized brushes unnecessary. Following characterization of the polymer layers by means of variable-angle spectroscopic ellipsometry (VASE) and static contact angle measurements, the lubrication properties of the PMAA brushes were investigated in macroscopic tribological experiments under low-contact-pressure, aqueous conditions. Results indicated that PMAA brushes have the potential to dramatically reduce sliding friction in an aqueous environment.

Introduction

Surface modifications by means of polymer brushes represent a very attractive tool for the tailoring and control of interfacial properties such as adhesion, friction, wettability, or biocompatibility.[1−3] Two principal experimental approaches are available to generate polymer brushes on solid substrates, namely "grafting to" and "grafting from".[4,5] While both approaches have their own unique characteristics, "grafting from" methods are known to be more suited to producing a high grafting density of chains because the polymers are generated *in situ* from a surface with a high density of initiating species. While "grafting to" approaches are more experimentally straightforward, they are restricted in terms of grafting densities, mainly due to the diffusion-limited adsorption of preformed polymers.[6] In recent years, numerous experimental strategies have been developed for the preparation of polymer brushes by means of "grafting from" methods.[4,7,8] Among them, controlled radical polymerization (CRP) strategies such as atom-transfer radical polymerization (ATRP),[9] nitroxide-mediated polymerization (NMP),[10−12] reversible addition−fragmentation transfer polymerization (RAFT),[13,14] and photoiniferter-mediated photopolymerization (PMP)[15,16] have gained considerable attention. The common feature of these methods is that the propagating chain continuously experiences activation−deactivation cycles to maintain a low radical concentration, which in turn minimizes irreversible chain termination. Therefore, CRP methods allow for the precise control of the polymer molecular weight and usually yield polymer brushes with low polydispersity. In addition, the preparation of block copolymer brushes becomes feasible as the active chain ends are typically preserved when a polymerization step is interrupted.

In this work, we have adapted the PMP method originally developed by Otsu et al.[15,16] to prepare poly(methacrylic acid) (PMAA) brushes on silicon surfaces, which are covered with native SiO_2. The PMP method is based on dithiocarbamate derivatives, which act as *ini*tiator, trans*fer* agent, and *ter*minating species (*iniferter*). Upon ultraviolet (UV) irradiation, the iniferter dissociates into a highly reactive radical as well as a noninitiating counter radical that reversibly terminates the propagation reaction. Advantages of the iniferter concept include the facile control of the polymerization reaction by means of irradiation time and UV intensity, the comparatively fast reaction kinetics compared to other CRP methods, and the fact that the polymerization can be easily performed at room temperature or below to avoid thermal polymerization of heat-sensitive monomers. Furthermore, the photoiniferter technique is compatible with aqueous media, it is suitable for micropatterning,[17,18] and it does not require any sacrificial initiator in the monomer solution. The latter is significant since it limits the formation of free polymers in the bulk solution and eliminates the need for extensive cleaning steps after brush formation.

The UV source employed in this work consisted of a recently developed, commercial high-power ultraviolet light-emitting diode,[19−22] and it was chosen for its distinct advantages compared to conventional UV sources. The sharp spectrum of these novel UV-LEDs (which are available in several different wavelengths) allows for a specific selection of the wavelength region according to the employed photoinitiating system and the reactive monomer. In comparison to conventional mercury lamps, the necessity for optical filters to block irradiation of undesired regions in the lamp spectrum is greatly reduced. This is advantageous since such filters frequently reduce the intensity in the desired wavelength region, leading to very poor energy efficiency and long irradiation times. The narrow spectrum of UV-LEDs is highly beneficial for controlled, surface-initiated polymerization reactions since the low-wavelength region of unfiltered mercury lamps generally induces polymerization of the monomer in the bulk solution. As a consequence, free polymer chains can become entangled within the growing polymer brush, which makes their controlled growth difficult and lengthy postcleaning processes unavoidable.

*Corresponding author. E-mail: nspencer@ethz.ch.

 Published on Web 09/23/2009

The polymer brushes prepared by means of UV-LED-induced photopolymerization were intended for the reduction of interfacial friction in an aqueous environment. While covalently attached polymer chains are readily removed during macroscopic sliding friction under contact pressures above 300−400 MPa,[23] the tribological experiments in this work aimed at aqueous lubrication under low contact pressures, for medical applications, for example. We have recently shown that strongly attached self-assembled monolayers (SAMs) and polymer brushes prepared by a "grafting to" approach represent promising aqueous lubrication additives under mild contact-pressure conditions.[23] While the previously employed surface modifications consisted of neutral, hydrophilic molecules with limited molecular weights and/or grafting densities, the introduction of charge, by means of weak polyelectrolyte brushes prepared with the PMP method, was expected to further enhance the lubricating ability of polymer brushes in an aqueous environment. In comparison to neutral hydrophilic brushes, polyelectrolyte brushes exhibit a very high osmotic pressure in aqueous environments of low ionic strengths, which renders them highly suitable for water-based lubrication purposes. For this reason, methacrylic acid (MAA) was chosen as a monomer, since it shows a high affinity toward water and because direct photopolymerization to PMAA brushes is feasible under carefully controlled reaction conditions. The preparation of PMAA brushes on Si/SiO_2 surfaces has been performed with a silane-derivatized dithiocarbamate iniferter developed by de Boer et al.[24] A number of polyelectrolyte brushes have been synthesized by "grafting from" approaches.[2,5,25−30] Since the carboxyl groups of acrylic acid-based monomers are prone to interact with metal catalysts, the synthesis of polyelectrolyte brushes by means of ATRP usually involves a hydrolysis step after the preparation of a neutral brush.[2,27,29,30] Therefore, the direct polymerization of polyelectrolyte brushes has typically been limited to either thermally induced approaches that require thorough cleaning steps after the brush synthesis, especially if a sacrificial initiator or free radicals are present in the monomer solution,[25,26] or the UV-induced photoiniferter approach.

In this work, a silane-derivatized dithiocarbamate iniferter was utilized to prepare PMAA brushes on Si/SiO_2 surfaces under UV irradiation. The combination of the photoiniferter-mediated photopolymerization with a UV-LED source appears to be ideally suited to the direct preparation of polyelectrolyte brushes with minimal free polymer formation during brush synthesis. Following characterization of the PMAA brushes by means of surface-analytical techniques, such as quartz crystal microbalance with dissipation monitoring (QCM-D), spectroscopic ellipsometry, and static contact-angle measurements, the PMAA brushes were demonstrated to enhance aqueous lubrication of Si/SiO_2 under low-contact-pressure conditions.

Experimental Section

Materials. *p*-(Chloromethyl)phenyltrimethoxysilane (ABCR, Germany), tetrahydrofuran (THF, 99.5% extra dry, Acros, Germany), methanol (Fluka, Switzerland), 2-propanol (Fluka, Switzerland), sulfuric acid (95−97%, Sigma-Aldrich, Germany), and hydrogen peroxide (30 wt % in water, VWR, Germany) were used as received. Sodium *N,N*-diethyldithiocarbamate (97%, Fluka, Switzerland) was recrystallized from methanol. Water was deionized with a GenPure filtration system (18.2 MΩ cm, TKA, Switzerland), and methacrylic acid (98%, Fluka, Switzerland) was first distilled under vacuum and subsequently passed through an alumina column (Sigma-Aldrich, Germany). The aqueous buffer solution employed for tribological experiments was prepared by adding 1 mM 4-(2-hydroxyethyl)-1-piperazineethanesulfonic acid (HEPES, BioChemika Ultra, Fluka, Switzerland) in pure water, and the solution pH was adjusted to a value of 7.4 by the addition of sodium hydroxide (NaOH, Fluka, Switzerland). The buffer is abbreviated as HEPES 0 throughout this article.

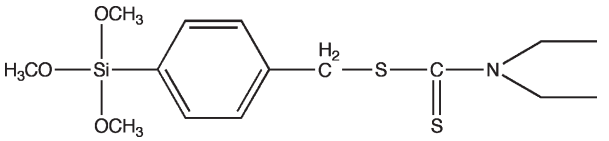

Figure 1. Chemical structure of the synthesized *N,N*-(diethylamino)dithiocarbamoylbenzyl(trimethoxy)silane (SBDC) photoiniferter.

Synthesis of the Photoiniferter, SBDC. The photoiniferter employed in this work (Figure 1) was synthesized according to a previously described protocol.[24] Briefly, *p*-(chloromethyl)-phenyltrimethoxsilane (CMPTMS) (1.48 g, 6 mmol) and sodium *N,N*-diethyldithiocarbamate (STC) (1.02 g, 6 mmol) were dissolved separately in 10 mL of dry THF before the STC solution was added slowly to the dissolved CMPTMS solution. After 3 h of stirring at room temperature, the solution was passed through a glass filter to remove the white NaCl precipitate, and THF was evaporated under reduced pressure. Prior to use, the photoiniferter (SBDC) was connected to a vacuum line for further drying ($p = 10^{-2}$ mbar, 4 h) and stored at −20 °C. The purified photoiniferter was obtained as a yellow viscous liquid and was characterized by ^{1}H NMR, and the data were in accordance with the values obtained by deBoer et al.[24]

Ultraviolet−Visible (UV−vis) Spectroscopy. The UV absorption spectra of both the SBDC photoiniferter and methacrylic acid were measured with a Cary 1 UV−vis spectrophotometer (Varian, Germany). The obtained spectra were taken as a reference for the selection of the spectral UV range in order to ensure effective initiation while avoiding polymerization of the monomer in solution.

Vapor Deposition of the Photoiniferter onto Si/SiO_2. Silicon wafers (P/B ⟨100⟩, Si-Mat Silicon Wafers, Germany) were cut into 20 mm × 20 mm pieces and ultrasonicated in 2-propanol twice for 15 min each time. Surface hydroxyl groups were generated on the silicon substrates by immersing the samples in a solution of concentrated sulfuric acid and 30 wt % hydrogen peroxide (H_2SO_4:H_2O_2 = 7:3), also known as piranha solution, for 60 min. (WARNING: piranha solution is very corrosive and must be handled with extreme caution; it reacts violently with organic materials and may not be stored in tightly closed vessels.) After rinsing the substrates with copious amounts of deionized water, they were dried with N_2 gas and immediately employed for surface modification.

In order to deposit the SBDC photoiniferter on the hydroxylated Si/SiO_2 substrates from the vapor phase, a 10 μL drop of the photoiniferter was placed in a desiccator, which was evacuated for 60 s with a rotary vane pump to evaporate residual solvent. Thereafter, the freshly cleaned Si/SiO_2 substrates were placed around the SBDC drop, and the desiccator was evacuated again, this time for 60 min ($p \approx 10^{-2}$ mbar). After closing the valve to the vacuum pump, the photoiniferter was allowed to adsorb onto the silicon oxide substrates for >48 h until atmospheric pressure was reached. Prior to UV-induced polymerization reactions, the photoiniferter-modified substrates were ultrasonicated in toluene for 2 min to remove physisorbed initiator before the initiator layer was characterized by variable angle spectroscopic ellipsometry and static contact-angle measurements.

This deposition method was chosen because the formation of a homogeneous SBDC layer, which is essential for the controlled and uniform growth of polymer brushes over large areas, is more readily achievable by the vapor-deposition approach than by adsorption from solution.[31]

Controlled Radical Photopolymerization by Means of a UV-LED. The grafting solution consisted of 10 vol % MAA in distilled water. Prior to polymerization, the solution was degassed in a glass flask by three alternating ultrasonication

(5 min) and vacuum (5 min) cycles. The photoiniferter-modified substrates were placed in a round-bottom Schlenk flask and continuously purged with N_2 gas for 5 min. Then, the previously degassed monomer solution was transferred to the sample-containing glass flask via a syringe under nitrogen atmosphere.

The high-power UV-LED (NCSU033A, NICHIA Corp., Japan) with a narrow emission spectrum at 365 ± 5 nm was mounted onto a printed circuit board (PCB) in series with a 5 Ω resistor and operated with a laboratory power supply. During operation, two axial fans were placed in front of the UV-LED to avoid a thermally related lifetime degradation of the diode. The distance from the LED surface to the sample was typically 25 mm, and the intensity at 365 nm was measured with a radiometer (UVX radiometer with UVX-36 sensor, UVP, Upland, CA). The LED-to-sample distance of 25 mm was determined by the size and the angle-dependent light intensity of the UV-LED to ensure a uniform exposure over the whole sample area (20 mm × 20 mm). As previously mentioned, the optical power output of the LED is conveniently related to the forward current. We applied a voltage of 8.5 V, resulting in a fixed forward current of 500 mA, which is the maximum for long-term operation recommended by the manufacturer. The photopolymerization reaction was initiated by turning the power supply up to this maximum value.

After the polymerization reaction, the samples were taken out of the monomer solution, rinsed with water for 60 s, and blown dry with N_2 gas before they were characterized by means of surface-analytical techniques.

Characterization of PMAA Brushes. The brush thickness in a dry state was determined with a variable-angle spectroscopic ellipsometer (VASE) (M-2000F, LOT Oriel GmbH, Darmstadt, Germany) at three different angles of incidence (65°, 70°, 75°). In order to ensure the formation of homogeneous polymer brushes over the whole sample area of 400 mm^2, five different spots were measured on each sample, from which the thickness values were determined via the analysis of a three-layer model (software WVASE32, LOT Oriel GmbH, Darmstadt, Germany). The spectral range considered was from 370 to 995 nm, and the dry film thickness of the PMAA brush layer was assumed to have a refractive index of 1.45.

Static water contact angles were determined by the sessile-drop method employing a Ramé-Hart goniometer (Ramé-Hart Instrument Co., Model-100, Netcong, NJ) at all stages of the surface-modification process, i.e., after cleaning of the SiO_2 substrates, after vapor deposition of the photoiniferter, and after photopolymerization of the PMAA brushes.

The photopolymerization kinetics of PMAA brushes on SiO_2 surfaces were monitored *in situ* by means of quartz-crystal microbalance experiments with dissipation monitoring (QCM-D) using a Q-Sense E4 instrument (Q-Sense, Västra Frölunda, Sweden). As substrates, AT-cut quartz crystals (fundamental resonance frequency = 5 MHz) with a sensor area of 1.54 cm^2 and a 50 nm silicon dioxide top layer (QSX 303, Q-Sense, Västra Frölunda, Sweden) were employed. The flexibility of the UV-LED setup allowed for the positioning of the LED at a 20 mm distance from the QCM cell with a transparent quartz glass window. The photoiniferter-modified quartz crystal resonator was immobilized inside the cell, and the sample-to-LED distance was maintained at 25 mm. The degassed monomer solution was injected into the QCM cell with a syringe.

Macroscopic tribological experiments were performed by recording the coefficient of friction (μ) at different sliding speeds with a conventional pin-on-disk tribometer (CSM Instruments, Peseux, Switzerland). The sliding partner of the PMAA brush-bearing substrates was a spherical-ended elastomeric poly(dimethylsiloxane) (PDMS) pin (Young's modulus = 1.4 MPa) with a diameter of 6 mm. Its high elasticity, its physiological inertness, and the straightforward fabrication make cross-linked PDMS ideally suitable as a model elastomer. In addition, it represents a technologically important material which displays a hydrophilic SiO_x surface layer after a 60 s air-plasma treatment (Harrick plasma cleaner/sterilizer, Ossining, NY).[32,33] The plasma-treated and thus oxidized PDMS pins are denoted as "ox-PDMS" pins throughout the article. The basic frictional properties of the PMAA brushes were tested at sliding speeds ranging from 0.25 to 10 mm/s. For each tribopair, 20 rotations were carried out at six different sliding speeds on a fixed sliding track (radius = 6 mm). The normal load was kept constant at 1 N. In order to analyze the stability of PMAA brush-bearing substrates under tribological stress, long-term pin-on-disk experiments (1000 rotations) were performed under 1 N normal load and at a sliding speed of 1 mm/s (Hertzian contact pressure ≈ 0.28 MPa).

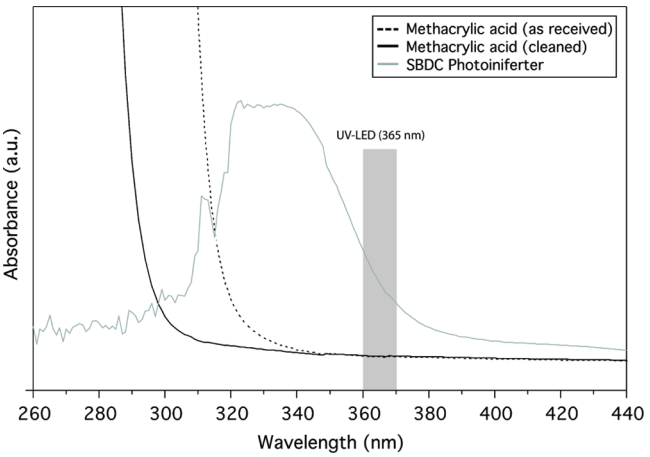

Figure 2. UV−vis spectra recorded from the SBDC photoiniferter and from the as-received as well as from the cleaned MAA monomer. The emission spectrum of the 365 nm UV-LED is indicated.

Results and Discussion

Ultraviolet−Visible (UV−vis) Absorption of Photoiniferter and Monomer. Figure 2 shows the UV−vis absorption spectra recorded from the SBDC photoiniferter as well as from as-received and cleaned methacrylic acid. While 10 μL of SBDC was dissolved in 1 mL of acetone and measured against an acetone reference, MAA was measured against air. As can be seen from Figure 2, significant UV absorption of the inhibitor-free, clean MAA starts around 300 nm, which is significantly lower than that of the as-received, stabilized MAA at around 320 nm. The SBDC photoiniferter shows an absorption maximum at ∼340 nm. Importantly, the monomer and the SBDC photoiniferter have distinct regions of UV absorption that do not overlap significantly, which is considered essential for a controlled surface-initiated polymerization process. In order to avoid polymerization of the monomer in solution, the spectral region of the UV source has to be matched with the absorption band of both the photoiniferter and the monomer; i.e., the UV source should have minimal emission in the region where the monomer shows significant UV absorption. Hence, careful selection of photoiniferter, monomer, and UV source are believed to significantly enhance the degree of control over the polymerization reaction. In this respect, the narrow emission spectrum of the 365 nm high-power UV-LED employed in this work is highly advantageous. The indicated emission spectrum of the UV-LED in Figure 2 shows that UV-induced polymerization of MAA in solution is unlikely to occur since the narrow emission spectrum of the UV-LED does not overlap with the UV absorption region of the monomer.

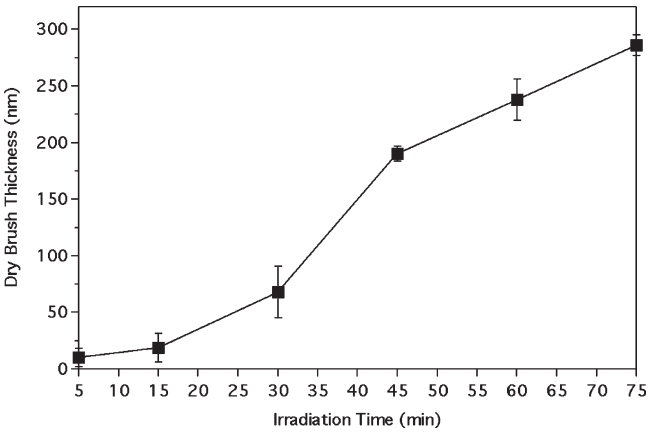

Figure 3. Characterization of the dry PMAA brush thickness as a function of irradiation time. The monomer solution consisted of 10 vol % MAA in water, and the 365 nm UV-LED intensity at the sample surface was 12 mW/cm^2. The lines serve as a guide to the eye.

Characterization of the Photoiniferter-Modified Substrates. After vapor deposition of the SBDC photoiniferter onto the Si/SiO_2 substrates and removal of any physisorbed material, the average static water contact angle was measured to be $68 \pm 3°$. This value is significantly higher than the contact angle of the cleaned SiO_2 surfaces ($5 \pm 3°$) and is consistent with the successful formation of a monomolecular photoiniferter layer on the silicon substrate. The obtained water contact angles are also in good agreement with previously reported values that were obtained following SBDC adsorption from solution.[34] In order to verify the homogeneity of the vapor-deposited photoiniferter layers, the ellipsometric thickness was determined at three distinct spots on each sample by assuming a refractive index of 1.45.[34] The average thickness obtained from at least 10 samples was determined to be 0.75 ± 0.06 nm. This value is significantly lower than the theoretical maximum thickness (1.3 nm) calculated by Rahane et al.[34] and suggests that the surface coverage is below that of a full monolayer. However, it has been previously shown that too high a concentration of surface radicals can lead to extensive termination reactions in surface-initiated polymerization approaches, thus favoring initiator densities below full-monolayer coverage.[35−37] The employed vapor deposition method can be applied to materials that are not compatible with organic solvents, such as polymeric substrates, and the probability of multilayer formation is significantly reduced when adsorbing trifunctional silanes from the vapor phase.[31,38]

Photopolymerization of Methacrylic Acid to Form PMAA Brushes. The photoinitiated grafting of PMAA brushes from SBDC-modified Si/SiO_2 substrates was performed with a 365 nm UV intensity of 12 mW/cm^2, measured at the sample surface. Figure 3 shows the dry ellipsometric thickness of the PMAA brushes obtained from 10 vol % monomer solutions as a function of irradiation time. As is visible from the dry thickness of the PMAA brushes, the UV-LED-initiated polymerization method allows for an effective control of the brush thickness with irradiation time. The PMAA brushes reach high dry thickness values after short irradiation times and with low monomer concentrations. Immersion of the samples in water for 24 h and subsequent drying did not noticeably change the brush thickness. The initial slow growth of the PMAA brushes is followed by a regime, in which the layer thickness increases very rapidly with irradiation time. For exposure times beyond 45 min, however, the brush growth was found to slow down. Similar growth characteristics have been found in earlier investigations using the same[34] or different[28,35−37] SIP methods. It is generally agreed that, in comparison to controlled/"living" polymerization reactions in solution, controlled SIP methods do not exhibit a "living" character.[34,36,37,39] The relatively low concentration of deactivating species, i.e., dithiocarbamyl radicals in this work, facilitates irreversible termination reactions, leading to a loss of reactive, surface-bound radicals. Hence, a saturation of the brush thickness at longer irradiation times is expected eventually. Since previous studies with the identical SBDC photoiniferter showed that the saturation of poly(methyl methacrylate) (PMMA) brush growth occurs significantly faster for higher monomer concentrations,[34] aqueous solutions with a fixed monomer concentration (10 vol % MAA) were employed in this work in order to ensure effective control over the PMAA brush thickness with irradiation time.

Many of the attractive properties of polymer brushes are closely related to the molecular weight of the individual polymer chains as well as to their proximity to each other on the surface, i.e., the surface grafting density. According to a simple model developed by Sofia et al.,[40] the surface grafting density can be estimated from ellipsometry data.

As illustrated in Figure 4, this model is based on close-packed unit cells with side lengths L and height d, each bearing one polymer chain. The volume V occupied by a single chain can be calculated from

$$V = L^2 d = \frac{M_w}{\rho_{dry} N_A} \tag{1}$$

where L^2 is the surface area occupied by a single chain, d is the dry thickness measured by ellipsometry, M_w is the molecular weight of a single chain, ρ_{dry} is the density of the dry monolayer, and N_A is Avogadro's number. In order to obtain the surface grafting density of the SBDC photoiniferter layer, for instance, eq 1 can be transformed to

$$\frac{1}{{L_{PI}}^2} = \left(\frac{d_{PI} \rho_{dry,PI} N_A}{M_{w,PI}} \right) \tag{2}$$

In addition to the ellipsometric thickness of the SBDC monolayer ($d_{PI} = 0.75 \pm 0.06$ nm) as well as the molecular weight ($M_{w,PI} = 317.5$ g/mol) of the individual chains, a constant value has to be assumed for the dry density ($\rho_{dry,PI}$) of the photoiniferter layer. Hence, the validity of this model is restricted to polymer monolayers in the brush regime that do not possess a significant density gradient along the chain. Assuming a value of 1 g/cm^3 for the density of the SBDC monolayer, its surface grafting density was estimated to be 1.42 chains/nm^2. On the basis of this data, it is possible to calculate the lower molecular weight limit of the PMAA chains after photopolymerization. Provided that all photoiniferter chains induce polymerization and grow with an identical rate, i.e., $L_{PI} = L_{PMAA}$, and by further assuming a dry density ($\rho_{dry,PMAA} = 1.12$ g/cm^3)[26] for the PMAA chains, eq 1 can be transformed to

$$M_{w,PMAA} = {L_{PMAA}}^2 d_{PMAA} \rho_{dry,PMAA} N_A \tag{3}$$

Table 1 shows the calculated minimum molecular weights of the PMAA brushes that were obtained from average dry ellipsometry thickness data of the photoiniferter monolayer and the PMAA brushes. Since the fraction of photoiniferter molecules that induces simultaneous polymer growth is

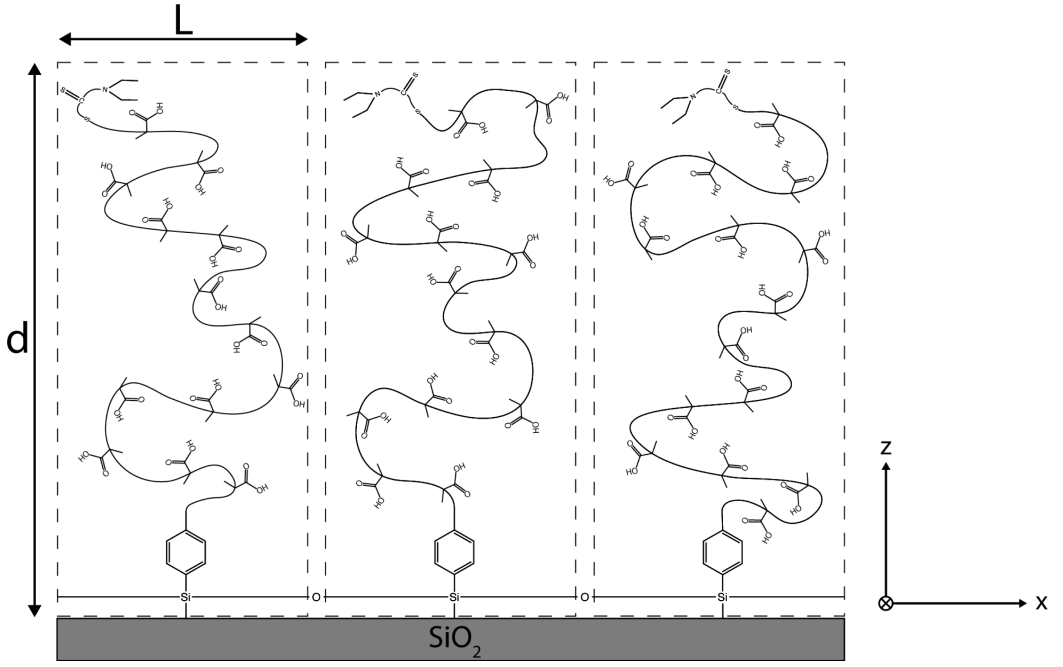

Figure 4. Two-dimensional model consisting of close-packed unit cells for the calculation of the surface grafting density and/or the molecular weight of surface-tethered polymer chains.

Table 1. Minimum Molecular Weights of the PMAA Brushes Prepared in This Work Based on Calculations from Eqs 1−3

irradiation time (min)	dry PMAA thickness (nm)	molecular weight (g/mol)
5	10	4 700
15	20	9 500
30	70	33 200
45	190	90 100
60	240	113 800
75	290	137 500

undoubtedly less than unity, it is clear that the molecular weight values of the PMAA brushes in Table 1 represent a lower limit.

Investigation of the *in Situ* PMAA Brush Growth by Means of QCM-D. The *in situ* observation of surface-initiated polymer brush growth by means of QCM has previously been reported in the literature.[35,41−44] It is a method particularly suited to UV-initiated polymerization. In order to ensure that the monomer solution does not polymerize in the absence of initiator, a blank SiO_2 crystal was first exposed to 10 vol % MAA in water and UV-irradiated for 30 min in a QCM-D setup. Figure 5 shows an increase of 6−7 Hz in the resonance frequency of the third overtone of the SiO_2 crystal upon UV exposure. This behavior has been observed previously[41] and is probably attributed to photoinduced noise. After the UV-LED was switched off after 30 min, the original resonance frequency values were retrieved, confirming that the 365 nm UV irradiation did not induce polymerization of the MAA monomer.

The *in situ* growth characteristics of PMAA brushes, determined by means of QCM-D experiments, are shown in Figure 6. After the UV-LED was switched on, the resonance frequency (black circles) increased slightly before a continuous decrease was observed. The onset of the negative frequency shift is believed to mark the start of PMAA brush polymerization since the decrease in resonance frequency can be attributed to an increase in the mass that is coupled to the QCM crystal. Up to ~25 min of brush growth, i.e., until ca. 40 min in Figure 6, the frequency of the third

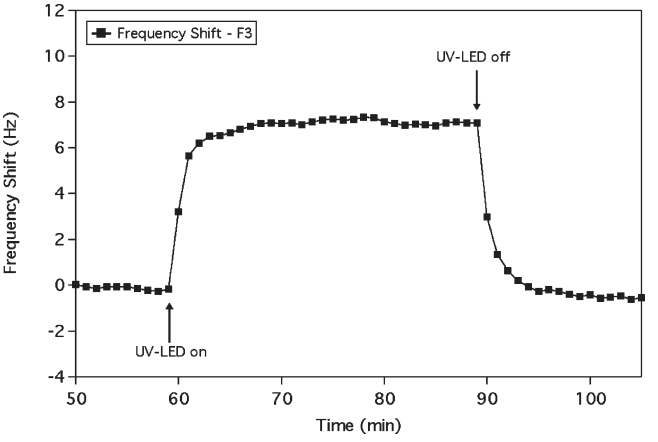

Figure 5. Shift in the resonance frequency of the third overtone of a SiO_2 QCM crystal in 10 vol % MAA solution upon exposure to 365 nm UV-LED irradiation.

overtone of the QCM crystal decreases almost linearly, suggesting a steady, continuous polymer growth. Prolonged irradiation was shown to lead to a higher polymerization rate. In contrast to the growth characteristics derived from ellipsometry data, the QCM-D experiment did not show a slower growth beyond 45 min of UV irradiation. This difference could be arising from that the difference in the physical quantity being probed by the two approaches, i.e., the total mass of the solvated polymer for QCM vs the thickness of the dry polymer for ellipsometry. QCM also detects incorporated solvent molecules and is therefore sensitive to configurational effects, i.e., the incorporation of more solvent in the brush than in mushroom configuration. Ellipsometry, on the other hand, simply provides the mass of polymer produced. The precise molecular nature of the transition in the QCM graph is, however, currently under investigation.

Our results suggest that a very slight degree of chain transfer, and consequent loss from the surface, occurs after longer irradiation times, since rinsing with fresh monomer

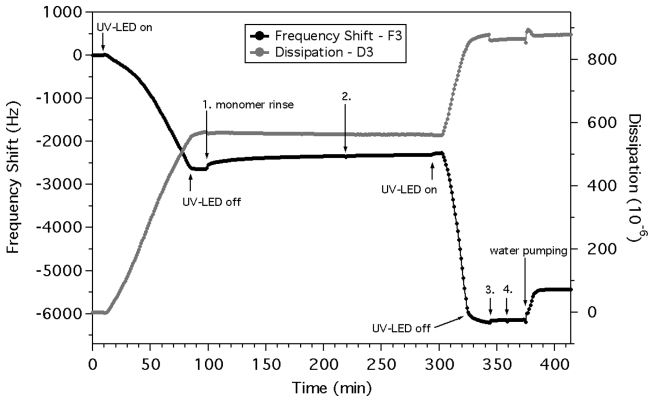

Figure 6. Frequency shift (black circles) and dissipation changes (gray circles) observed in QCM-D experiments during surface-initiated, *in situ* polymerization of PMAA brushes from 10 vol % monomer solutions in water. After a first polymerization step, the QCM cell was rinsed with fresh monomer solution (after 100 min) before the UV-LED was switched on again (after 290 min) to induce a second polymerization step. After the UV source was switched off (after 325 min), the cell was rinsed with fresh monomer twice before pure water was continuously pumped through the system in order to remove unbound polymer.

solution after the UV-LED was switched off (after 85 min in Figure 6) led to a minor decrease in the mass coupled to the QCM crystal from −2700 Hz after 100 min to −2380 Hz after 290 min in Figure 6. In contrast, the dissipation, which represents the sum of all energy losses per oscillation cycle, was almost constant during that period. It is believed that unbound polymer chains, which evolved from chain transfer reactions, can become entangled inside the brush and consequently reduce the mobility of individual brush chains. From the point of view of tribology, the viscoelastic properties of polymer brushes are extremely important since the solvation of the brush leads to a fluidlike cushion layer, which promotes facile sliding.

With the SI-PMP technique employed in this work, the active chain ends should be preserved after the polymerization step. In order to verify that, the UV-LED was switched on again (after 290 min) after stable resonance frequencies were obtained. As visible from the frequency and dissipation shifts after 300 min in Figure 6, the photopolymerization of PMAA brushes continues ∼10 min after the UV-LED was switched on for the second time. Compared to the initial step, the second photopolymerization reaction occurs at a significantly faster rate, indicated by the steep decrease of the resonance frequency from −2300 to −6000 Hz within 25 min. After the UV-LED was switched off, the frequency continued to show a slight shift toward lower values, suggesting that the polymerization did not stop completely after the UV source was turned off. This is in contrast to the observations from the first polymerization step and indicates that the concentration of chain-terminating species is somewhat lower. It is thus very likely that fewer polymer chains grow much faster compared to the initial polymerization step. This is also reflected in the dissipation curve of the third overtone frequency (gray circles), which only increases by $\approx 290 \times 10^{-6}$ whereas the first polymerization led to a 560×10^{-6} increase in dissipation. The relatively low increase in dissipation compared to the high frequency shift during the second polymerization step also suggests that the growing chains are entangled inside the existing brush.

The generation of polymer in solution is very limited during the second polymerization step, as indicated by the small increase in the resonance frequency and decrease in the dissipation, respectively, after rinsing with fresh monomer (rinsing steps 3 and 4 in Figure 6). After ∼375 min, deionized water was continuously pumped through the QCM cell in order to remove potential unanchored PMAA chains as well as to see differences in the hydration properties of the brush. The fast saturation of both the resonance frequency and the dissipation values suggest that the presence of unbound polymer chains is very limited during the UV-LED-induced photopolymerization method employed in this work. Hence, simple rinsing steps after the polymerization reaction appear to be sufficient to obtain well-defined PMAA brushes. While the frequency shifts toward higher values under a continuous flow of water, the dissipation was found to increase slightly. The higher frequency, indicative of a lower mass coupled to the QCM crystal, is associated with the exchange of the heavier methacrylic acid ($M_w = 86.10$ g/mol) with water ($M_w = 18.02$ g/mol), rather than with the removal of polymer chains.

Thermally induced polymerization of the monomer could be excluded during photopolymerization, since the UV-LED did not induce any temperature increase in the QCM-D setup. The temperature which was set to 25 °C varied by less than 0.01 °C in the course of the experiment. Furthermore, from the fact that UV exposure of the monomer itself did not induce polymerization (Figure 5), we suspect that chain transfer to monomer is occurring at later stages of the polymerization. Free polymer formed in the course of polymerization cannot be distinguished in a QCM-D experiment if the chains are entangled inside the brush or if the polymer significantly increases the viscosity of the monomer solution. The rinsing step after switching off the UV-LED, however, showed that some free polymer chains are present in solution. Unfortunately, most other studies presenting QCM data do not show such a rinsing step, although this would help to effectively distinguish between surface-tethered and unbound polymer.

Hydrophilicity of PMAA Brushes. Since the PMAA brushes prepared in this work were intended for aqueous tribology, the water compatibility of the surfaces is of particular interest. Therefore, the hydrophilicity of the PMAA brushes was measured by means of static contact-angle experiments. In comparison to the photoiniferter-modified substrates with a static water contact angle of 68 ± 3°, the PMAA brush-bearing samples exhibited average contact-angle values of 49 ± 7°, irrespective of the brush lengths. The water contact angles of hydrophilic polymer brushes have previously been found to be finite and nearly independent of the molecular weight, which has been attributed to the fact that the polymer chains can bridge the solvent−vapor interface.[45] Since the active chain ends were preserved during the PMAA polymerization reaction (Figure 6), the diethyldithiocarbamate-terminating groups are likely to contribute to the hydrophobic character of the PMAA-modified substrates in air. Nevertheless, it is expected that PMAA brushes can provide a lubricious interface in an aqueous environment because they exhibit a large number of ionizable carboxyls along their backbone.

Macroscopic Aqueous Lubrication Properties of PMAA Brushes. If the relative sliding speed between two contacting bodies is low or if the applied normal load is high, the lubricant is squeezed out of the contact area. This behavior is even more pronounced for low-viscosity fluids such as water and normally results in high interfacial friction and wear. The presence of a protecting polymer brush has been shown to greatly reduce the friction in this so-called "boundary-lubrication regime".[1,46,47] While direct contact and adhesion between asperities can be avoided for polymer brush-bearing surfaces, the incorporation of lubricant molecules

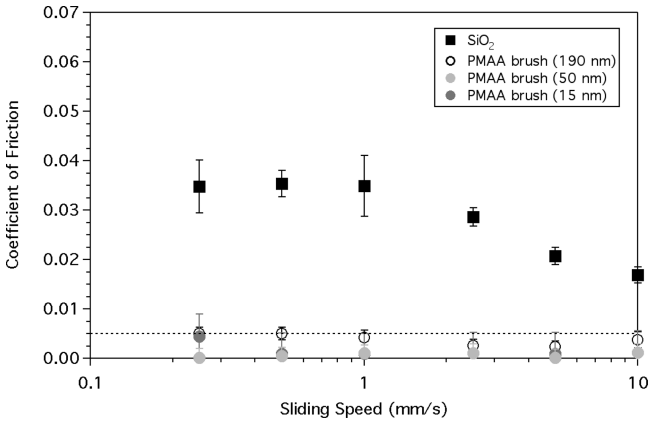

Figure 7. Pin-on-disk speed-dependence measurements obtained from PMAA brushes and from bare Si/SiO_2 substrates against an oxidized PDMS pin in HEPES 0 (normal load: 1 N). Dotted line indicates the sensitivity limit of the tribometer.

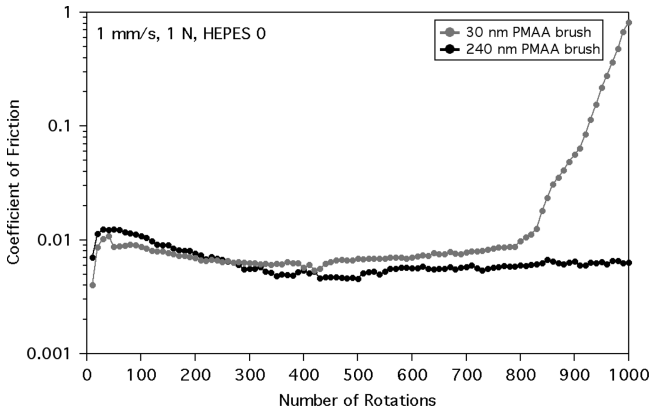

Figure 8. Long-term pin-on-disk experiments involving PMAA brushes with two distinct brush heights (30 and 240 nm). The shorter brush (gray circles) did not sustain the applied tribological stress (1 N normal load, 1 mm/s sliding speed) for 1000 rotations, while the 240 nm PMAA samples displayed very low friction coefficients throughout the entire experiment.

inside the brush additionally creates a fluidlike layer of low shear strength and thus facilitates sliding.[46]

We have previously demonstrated that hydrophilic polymer brushes can effectively reduce the interfacial friction in an aqueous environment under low-sliding-speed conditions.[48,49] In those studies, we employed "grafting to" approaches to generate polymer brushes on a variety of substrates. By applying the "grafting from" method described in this work, the formation of high-surface-density polyelectrolyte brushes became feasible. To date, only little experimental work has been dedicated to the macroscopic lubrication properties of polymer brushes prepared with a "grafting from" method.[50,51]

In many practical lubrication applications, high contact pressures on the order of 1 GPa are routinely encountered. Under such conditions, even strongly attached polymer brushes are easily removed during macroscopic sliding experiments. The reduction of the contact pressure by means of a soft rather than a rigid slider is usually sufficient for enabling the polymer brushes to sustain the tribological stress. The macroscopic pin-on-disk data obtained from different PMAA brushes against oxidized PDMS pins in HEPES 0 are presented in Figure 7. For comparison purposes, results from a bare Si/SiO_2 sample are included. From the coefficient of friction (μ) vs sliding speed plots, it is clear that clean, hydrophilic silica surfaces exhibit moderately good aqueous lubrication properties under low contact pressure conditions, especially at relatively high sliding speeds ($\mu \approx 0.017$ at 10 mm/s). Toward lower sliding speeds, i.e., in the boundary regime, these surfaces are not capable of maintaining a sufficiently thick lubricant film, which is manifested in the increase of the coefficient of friction by a factor of 2 ($\mu \approx 0.035$ at 0.25 mm/s).

In this respect, the PMAA brush-bearing surfaces were found to serve as very effective surfaces under boundary-lubrication conditions in water. All tested brushes with a dry ellipsometric thickness ranging from 15 to 190 nm showed friction coefficients below the sensitivity limit ($\mu = 0.005$) of the employed macrotribometer at the load employed. This resolution limit is indicated with a dotted line in Figure 7, and the plot shows that these low friction values were maintained over the entire sliding-speed range. Therefore, it was not possible to effectively distinguish the different PMAA brushes by their lubricating properties in HEPES 0. The results suggest that all PMAA brushes were able to create a highly hydrated, fluidlike interface, rendering these surface modifications highly compatible for aqueous lubrication purposes at neutral pH.

In order to test the stability of the PMAA brushes in longer term pin-on-disk experiments, two samples with different brush heights (30 and 240 nm dry thickness) were exposed to tribological stress for 1000 rotations under 1 N normal load and a sliding speed of 1 mm/s. The brush-bearing samples were immersed in HEPES 0 for 10 min prior to the pin-on-disk experiment. Figure 8 shows that the μ values from the shorter brush reach a maximum of 0.01 during initial rotations before the friction decreases to $\mu \approx 0.006$ after 200 rotations. The frictional response during that period is explained by the relatively slow complete hydration of the brush. Since the static water contact angles of the dry brushes are rather high, it seems likely that the complete hydration of PMAA chains takes some time. Apparently, the immersion of the brushes into the aqueous lubricant prior to pin-on-disk experiments is not sufficient for a complete hydration, but the samples become more hydrated under the influence of tribological stress. Between 200 and 450 rotations, the coefficient of friction from the 30 nm PMAA brush is nearly constant, before a slight but continuous increase in friction could be observed. After 790 rotations, the μ values increase drastically up to $\mu \approx 1.0$. Hence, the short PMAA brushes did not sustain the tribological stress for 1000 rotations.

When the identical long-term pin-on-disk experiment was performed with the longer PMAA brush (240 nm dry thickness), the coefficient of friction decreases from initially $\mu = 0.01$ to values below the detection limit of the pin-on-disk tribometer ($\mu = 0.005$) within the first 400 rotations. This behavior was again attributed to a continuous hydration process of the thick PMAA brush, the highest lubricity being expected after maximum swelling. In comparison to the short brush, the friction coefficients from the 240 nm PMAA sample were found to decrease over a longer period of time, which is believed to be due to a prolonged hydration process of brushes with a higher thickness. The next 200 rotations are characterized by undetectably low friction coefficients, after which the μ values seem to increase slightly and stabilize at around $\mu = 0.006$ for the remaining 400 rotations. In comparison to the speed-dependence experiments in Figure 7, where the undetectably low friction was observed at the initial sliding speed of 10 mm/s, the swelling of both short and long brushes, i.e., the fluid uptake, appears to be significantly slower at a sliding speed of 1 mm/s. Nonetheless, the

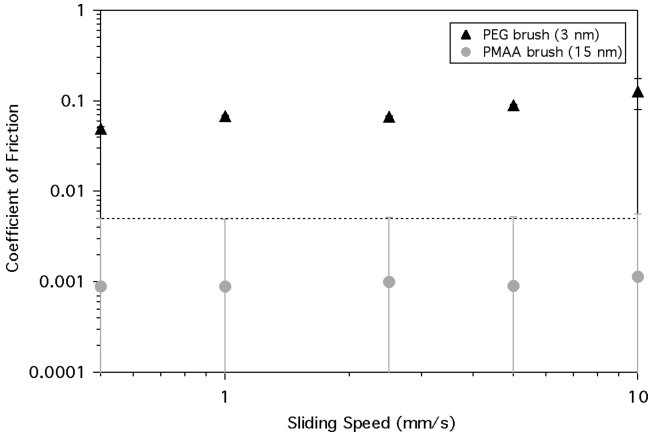

Figure 9. Comparison of μ vs sliding speed plots between 15 nm PMAA brushes and 3 nm PEG (5000) monolayers, which have been prepared via "grafting from" and "grafting to" methods, respectively. The molecular weight of individual polymer chains was expected to be of the same order of magnitude for both brushes.

obtained friction coefficients from both brushes were well below $\mu = 0.01$ over several hundred rotations, with the difference that the 30 nm PMAA brush did not show the superior long-term stability of the 240 nm PMAA samples.

In Figure 9, a comparison is made between the frictional properties of a 15 nm PMAA brush and a 3 nm PEG (5000) monolayer. On the basis of the ellipsometric dry thickness values from the 15 nm PMAA brush, its molecular weight was determined to be 6350 g/mol, which is in the range of the employed PEG chains (5000 g/mol). The fact that the dry thickness of the PMAA brush is 5 times higher than that of the PEG monolayer can be explained by the differences in surface grafting density due to the different preparation methods; i.e., the PEG monolayer was obtained by the adsorption of PEG-silane (5000) molecules on Si/SiO_2 substrates from toluene solution—a "grafting to" method. Since PEG-based polymer brushes have previously proven to be very effective aqueous boundary lubricant additives,[48,49,52] it was interesting to compare them directly with PMAA brushes. Even though the PEG (5000) monolayer showed very low and extremely stable friction coefficients of around 0.05 over the tested speed range (10−0.5 mm/s), the values obtained from the 15 nm PMAA brush were again found to be below the detection limit ($\mu = 0.005$) of the tribometer, indicated by the dotted line in Figure 9. This also explains the apparently high standard deviations in the μ values obtained from PMAA brushes compared to those from PEG monolayers, for which friction was 1 order of magnitude *above* the sensitivity limit. The superior lubrication properties of PMAA brushes compared to PEG monolayers at neutral solution pH are attributed to a number of factors. First, the PMAA brushes prepared by the "grafting from" method show a significantly higher grafting density than that of the PEG monolayers. Second, the density of hydrophilic moieties (−COOH) inside the brush is higher for PMAA brushes, and their deprotonation at neutral solution pH is expected to enhance the swelling of polyelectrolyte brushes. The hydrated thickness of the boundary lubricant is also important with regard to the surface roughness of the tribopair. If the hydrated brush length is significantly larger than the roughness of the tribopair, direct asperity contact between the sliding surfaces can be avoided, even if only one surface is bearing a polymer brush. A further effect that may reduce the friction between PMAA brushes against oxidized PDMS pins results from electrostatic repulsion between the two sliding surfaces at neutral pH. The schematic in Figure 10 illustrates the presumed tribological interface formed by a PMAA brush against an ox-PDMS in an aqueous environment at neutral pH.

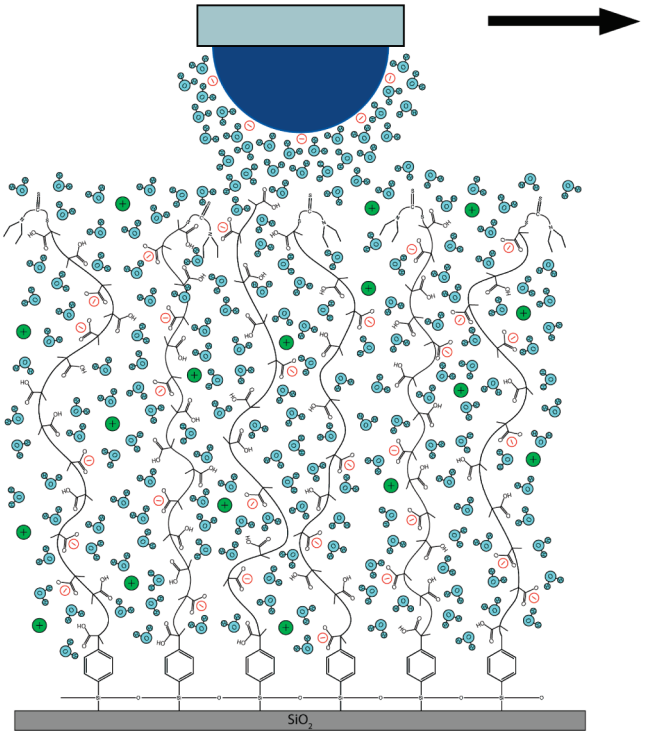

Figure 10. Presumed tribological interface between a highly hydrated PMAA brush and an ox-PDMS slider in an aqueous environment of neutral pH.

Conclusions

We reported the controlled growth of poly(methacrylic acid) brushes on Si/SiO_2 surfaces via a photoinduced "grafting from" approach. The employment of a relatively novel UV-LED setup allowed for the preparation of polymer brushes with a high dry thickness within comparatively short reaction times and low monomer concentrations. By careful purification of monomer and choice of photoinitiating system and UV source, the polymerization of monomer in solution could be suppressed, which rendered lengthy cleaning steps of the formed polymer brushes unnecessary. In this context, we consider the utilization of UV-LEDs to be very advantageous, since the narrow emission spectrum of the LED could be selected in a region where the monomer does not absorb UV irradiation. In conventional mercury arc UV lamps, for instance, the lower regions of the emission spectrum have to be filtered out in order to avoid polymerization of the monomer in solution. Besides the fact that optical filters often drastically reduce the intensity in the desired wavelength region, such lamps have to be effectively cooled to avoid heating of the monomer solution and associated thermally induced polymerization.

After the preparation of the PMAA brushes, their lubrication ability under low contact pressures was tested in a neutral aqueous solution. It was shown that the macroscopic friction between polyelectrolyte brushes of different molecular weights and soft, hydrophilic ox-PDMS pins was below the detection limit of the employed pin-on-disk tribometer over the entire speed range tested. While the PMAA brushes could not be distinguished with μ vs sliding speed plots, the long-term stability of short 15 nm PMAA brushes was shown to be inferior to long brushes (240 nm dry thickness). A further comparison between

PMAA brushes and PEG monolayers, of which the latter represent well-known aqueous boundary lubricants that are generally adsorbed on surfaces via "grafting to" methods, showed that PMAA brushes display significantly lower friction under aqueous lubrication conditions. Besides the higher grafting densities of the PMAA compared to PEG layers, enhanced swelling of the polyelectrolyte brushes in neutral aqueous media and additional electrostatic repulsion against the oxidized PDMS slider are presumably responsible for the significantly decreased frictional response.

In summary, we expect that strongly attached polyelectrolyte brushes hold great potential as effective surfaces for aqueous boundary lubrication under low contact pressures. To this end, the controlled polymerization of dense polymer brushes via the employed photopolymerization method is believed to serve as a versatile tool for the specific fabrication of ultralow-friction surfaces.

Acknowledgment. The authors are grateful to Drs. Andreas Mühlebach (Ciba Specialty Chemicals), Rupert Konradi (BASF), and Erik Reimhult (ETH Zurich) for useful discussions. The financial assistance of the ETH Research Commission is greatly appreciated.

References and Notes

(1) Raviv, U.; Giasson, S.; Kampf, N.; Gohy, J. F.; Jerome, R.; Klein, J. *Nature* **2003**, *425* (6954), 163–165.
(2) Dong, R.; Krishnan, S.; Baird, B. A.; Lindau, M.; Ober, C. K. *Biomacromolecules* **2007**, *8* (10), 3082–3092.
(3) Limpoco, F. T.; Advincula, R. C.; Perry, S. S. *Langmuir* **2007**, *23* (24), 12196–12201.
(4) Zhao, B.; Brittain, W. J. *Prog. Polym. Sci.* **2000**, *25* (5), 677–710.
(5) Ruhe, J.; Ballauff, M.; Biesalski, M.; Dziezok, P.; Grohn, F.; Johannsmann, D.; Houbenov, N.; Hugenberg, N.; Konradi, R.; Minko, S.; Motornov, M.; Netz, R. R.; Schmidt, M.; Seidel, C.; Stamm, M.; Stephan, T.; Usov, D.; Zhang, H. N. *Polyelectrolytes Defined Mol. Archit. I* **2004**, *165*, 79−150.
(6) Ruhe, J. *Polymer Brushes: On the Way to Tailor-Made Surfaces*; Wiley-VCH: New York, 2004; pp 1−31.
(7) Edmondson, S.; Osborne, V. L.; Huck, W. T. S. *Chem. Soc. Rev.* **2004**, *33* (1), 14–22.
(8) Tsujii, Y.; Ohno, K.; Yamamoto, S.; Goto, A.; Fukuda, T. *Surf.-Initiated Polym. I* **2006**, *197*, 1−45.
(9) Wang, J. S.; Matyjaszewski, K. *Macromolecules* **1995**, *28* (23), 7901–7910.
(10) Hawker, C. J.; Bosman, A. W.; Harth, E. *Chem. Rev.* **2001**, *101* (12), 3661–3688.
(11) Benoit, D.; Chaplinski, V.; Braslau, R.; Hawker, C. J. *J. Am. Chem. Soc.* **1999**, *121* (16), 3904–3920.
(12) Hawker, C. J.; Barclay, G. G.; Orellana, A.; Dao, J.; Devonport, W. *Macromolecules* **1996**, *29* (16), 5245–5254.
(13) Chiefari, J.; Chong, Y. K.; Ercole, F.; Krstina, J.; Jeffery, J.; Le, T. P. T.; Mayadunne, R. T. A.; Meijs, G. F.; Moad, C. L.; Moad, G.; Rizzardo, E.; Thang, S. H. *Macromolecules* **1998**, *31* (16), 5559–5562.
(14) Moad, G.; Rizzardo, E.; Thang, S. H. *Aust. J. Chem.* **2005**, *58* (6), 379–410.
(15) Takayuki Otsu, M. Y. *Makromol. Chem., Rapid Commun.* **1982**, *3* (2), 127–132.
(16) Takayuki Otsu, M. Y. T. T. *Makromol. Chem., Rapid Commun.* **1982**, *3* (2), 133–140.
(17) Nakayama, Y.; Matsuda, T. *Macromolecules* **1996**, *29* (27), 8622–8630.
(18) Luo, N.; Metters, A. T.; Hutchison, J. B.; Bowman, C. N.; Anseth, K. S. *Macromolecules* **2003**, *36* (18), 6739–6745.
(19) Morita, D.; Sano, M.; Yamamoto, M.; Matoba, K.; Yasutomo, K.; Akaishi, K.; Kasai, Y.; Nagahama, S.; Mukai, T. In 365-mn ultraviolet light emitting diodes with an output power of over 400 mW, Conference on Quantum Sensing and Nanophotonic Devices, San Jose, CA, Jan 25−29, 2004; Razeghi, M., Brown, G. J., Eds.; **2004**; pp 415−421.
(20) Morita, D.; Yamamoto, M.; Akaishi, K.; Matoba, K.; Yasutomo, K.; Kasai, Y.; Sano, M.; Nagahama, S.; Mukai, T. *Jpn. J. Appl. Phys., Part 1* **2004**, *43* (9A), 5945–5950.
(21) Morita, D.; Sano, M.; Yamamoto, M.; Nonaka, M.; Yasutomo, K.; Akaishi, K.; Nagahama, S.; Mukai, T. In Over 200 mW on 365 nm ultraviolet light emitting diode of GaN-free structure, 5th International Conference on Nitride Semiconductors (ICNS-5), Nara, Japan, May 25−30, 2003; **2003**, pp 114−117.
(22) Morita, D.; Sano, M.; Yamamoto, M.; Murayama, T.; Nagahama, S.; Mukai, T. *Jpn. J. Appl. Phys., Part 2* **2002**, *41* (12B), L1434–L1436.
(23) Lee, S.; Heeb, R.; Venkataraman, N. V.; Spencer, N. D. *Tribol. Lett.* **2007**, *28* (3), 229–239.
(24) de Boer, B.; Simon, H. K.; Werts, M. P. L.; van der Vegte, E. W.; Hadziioannou, G. *Macromolecules* **2000**, *33* (2), 349–356.
(25) Biesalski, M.; Johannsmann, D.; Ruhe, J. *J. Chem. Phys.* **2002**, *117* (10), 4988–4994.
(26) Konradi, R.; Ruhe, J. *Macromolecules* **2004**, *37* (18), 6954–6961.
(27) Parnell, A. J.; Martin, S. J.; Dang, C. C.; Geoghegan, M.; Jones, R. A. L.; Crook, C. J.; Howse, J. R.; Ryan, A. J. *Polymer* **2009**, *50* (4), 1005–1014.
(28) Jain, P.; Dai, J. H.; Baker, G. L.; Bruening, M. L. *Macromolecules* **2008**, *41* (22), 8413–8417.
(29) Matyjaszewski, K.; Miller, P. J.; Shukla, N.; Immaraporn, B.; Gelman, A.; Luokala, B. B.; Siclovan, T. M.; Kickelbick, G.; Vallant, T.; Hoffmann, H.; Pakula, T. *Macromolecules* **1999**, *32* (26), 8716–8724.
(30) Wu, T.; Gong, P.; Szleifer, I.; Vlcek, P.; Subr, V.; Genzer, J. *Macromolecules* **2007**, *40* (24), 8756–8764.
(31) Ashurst, W.R.; Carraro, C.; Maboudian, R. *IEEE Trans. Device Mater. Reliab.* **2003**, *3* (4), 173–178.
(32) Fritz, J. L.; Owen, M. J. *J. Adhes.* **1995**, *54* (1−2), 33–45.
(33) Efimenko, K.; Wallace, W. E.; Genzer, J. *J. Colloid Interface Sci.* **2002**, *254* (2), 306–315.
(34) Rahane, S. B.; Kilbey, S. M.; Metters, A. T. *Macromolecules* **2005**, *38* (20), 8202–8210.
(35) Niwa, M.; Date, M.; Higashi, N. *Macromolecules* **1996**, *29* (11), 3681–3685.
(36) Xiao, D. Q.; Wirth, M. J. *Macromolecules* **2002**, *35* (8), 2919–2925.
(37) Kim, J. B.; Huang, W. X.; Miller, M. D.; Baker, G. L.; Bruening, M. L. *J. Polym. Sci., Part A: Polym. Chem.* **2003**, *41* (3), 386–394.
(38) Jung, G. Y.; Li, Z. Y.; Wu, W.; Chen, Y.; Olynick, D. L.; Wang, S. Y.; Tong, W. M.; Williams, R. S. *Langmuir* **2005**, *21* (4), 1158–1161.
(39) Rahane, S. B.; Kilbey, S. M.; Metters, A. T. *Macromolecules* **2008**, *41* (24), 9612–9618.
(40) Sofia, S. J.; Premnath, V.; Merrill, E. W. *Macromolecules* **1998**, *31* (15), 5059–5070.
(41) Nakayama, Y.; Matsuda, T. *Macromolecules* **1999**, *32* (16), 5405–5410.
(42) Benetti, E. M.; Reimhult, E.; de Bruin, J.; Zapotoczny, S.; Textor, M.; Vancso, G. J. *Macromolecules* **2009**, *42* (5), 1640–1647.
(43) Moya, S. E.; Brown, A. A.; Azzaroni, O.; Huck, W. T. S. *Macromol. Rapid Commun.* **2005**, *26* (14), 1117–1121.
(44) Kurosawa, S.; Aizawa, H.; Talib, Z. A.; Atthoff, B.; Hilborn, J. *Biosens. Bioelectron.* **2004**, *20* (6), 1165–1176.
(45) Stuart, M. A. C.; de Vos, W. M.; Leermakers, F. A. M. *Langmuir* **2006**, *22* (4), 1722–1728.
(46) Klein, J. *Annu. Rev. Mater. Sci.* **1996**, *26*, 581–612.
(47) Lee, S.; Spencer, N. D. *Science* **2008**, *319* (5863), 575–576.
(48) Lee, S.; Muller, M.; Heeb, R.; Zurcher, S.; Tosatti, S.; Heinrich, M.; Amstad, F.; Pechmann, S.; Spencer, N. D. *Tribol. Lett.* **2006**, *24* (3), 217–223.
(49) Lee, S.; Iten, R.; Muller, M.; Spencer, N. D. *Macromolecules* **2004**, *37* (22), 8349–8356.
(50) Kobayashi, M.; Terayama, Y.; Hosaka, N.; Kaido, M.; Suzuki, A.; Yamada, N.; Torikai, N.; Ishihara, K.; Takahara, A. *Soft Matter* **2007**, *3* (6), 740–746.
(51) Sakata, H.; Kobayashi, M.; Otsuka, H.; Takahara, A. *Polym. J.* **2005**, *37* (10), 767–775.
(52) Lee, S.; Spencer, N. D. Achieving Ultralow Friction by Aqueous, Brush-Assisted Lubrication. In *Superlubricity*; Erdemir, A., Martin, J.-M., Eds.; Elsevier: Amsterdam, 2007; pp 365−396.